On potential causes for an under-estimated global ocean heat content trend in CMIP3 models

W. Cai,[1] T. Cowan,[1] J. M. Arblaster,[2,3] and S. Wijffels[4]

Received 17 June 2010; accepted 28 July 2010; published 14 September 2010.

[1] Trends in global oceanic heat content (OHC) over the late 20th century as simulated by climate models that incorporate all radiative forcing factors are smaller than the observed, but the causes are not clear. Given the cooling effect associated with increasing anthropogenic aerosols and natural forcing (i.e., volcanic aerosols), we examine their respective roles in the simulated global OHC trend and the associated ocean temperature structure, using targeted experiments from two models, designed to separate the individual impacts of these forcing components. We show that it is more likely that the indirect effect of aerosols, not volcanic aerosols alone, is the reason for the bulk of weaker modelled OHC trends. Further, anthropogenic aerosols are essential for simulating the structure of the observed temperature changes, including a concentrated cooling in the Southern Hemisphere subtropical latitudes, consistent with a more stable global Conveyer, a greater strengthening of the subtropical gyre circulation, and a stronger Southern Annular Mode trend in targeted experiments with anthropogenic aerosol forcing. **Citation:** Cai, W., T. Cowan, J. M. Arblaster, and S. Wijffels (2010), On potential causes for an under-estimated global ocean heat content trend in CMIP3 models, *Geophys. Res. Lett.*, *37*, L17709, doi:10.1029/2010GL044399.

1. Introduction

[2] An ensemble mean of 20th century model experiments (submitted as part of the Coupled Model Intercomparison Project Phase 3 (CMIP3)) forced with all forcing factors (ALL) such as time-varying well-mixed greenhouse gases, anthropogenic and volcanic aerosols, ozone depletion, and solar irradiance, produces a linear trend in the upper 300m OHC over 1961–1999 that is 28% smaller than the observed [*Domingues et al.*, 2008]. The weak OHC trend extends to the upper 2000 m, as seen in an ensemble mean over seven CMIP3 models (brown dots, Figure 1a), similarly forced by all forcing factors (see Table S1 of the auxiliary material, for CMIP3 model details); the linear trend of this CMIP3 ALL ensemble is 0.24×10^{22} J yr^{-1}, 60% of the observed, which is 0.40×10^{22} J yr^{-1} (orange square, Figure 1a) based on measurements from 1960–2007 [*Wijffels et al.*, 2008].[1] The weak upper 2000m OHC linear trend is confirmed from another CMIP3 ensemble used by *Domingues et al.* [2008], which is about 53% of the observed, based on 18 experiments from five models (figure not shown).

[3] It is important to understand the underlying cause of the underestimated global OHC trend so as to increase confidence in climate projections using these models. Given that both anthropogenic aerosols [e.g., *Liepert et al.*, 2004; *Nazarenko and Menon*, 2005; *Cai et al.*, 2006] and the natural forcing (volcanic aerosols and solar irradiance combined) [e.g., *Domingues et al.*, 2008; *Stenchikov et al.*, 2009] induce a cooling, are these cooling effects systematically overestimated by models? What is their respective role in driving the structure of the ocean temperature changes and trends in the global OHC?

[4] The design of CMIP3 model experiments is not tailored for resolving the above issues. Although all the experiments from each model incorporate the forcing of increasing anthropogenic aerosols, there are no corresponding experiments that are forced without increasing anthropogenic aerosols. Furthermore, some include only the direct aerosol effect, whereas others incorporate both the direct and the indirect aerosol effect, which are sources of great uncertainty. The indirect effect refers to a mechanism by which aerosols modify the microphysical and radiative properties, amount and lifetime of clouds [*Forster et al.*, 2007]. Likewise, there are no such experiments that "cleanly" separate the impact of natural forcing. Highlighting the importance of such a clean separation is the fact that averaged over another CMIP3 subgroup containing 10 models with anthropogenic forcing factors (ANT) only (i.e., without natural forcings (NAT)) the ensemble-mean upper-2000 m OHC trend is almost 70% larger than the observed (red dots, Figure 1b). Clearly, the difference between the CMIP3 ALL and ANT ensembles ($\sim 0.43 \times 10^{22}$ J yr^{-1} over the upper 2000 m) can not be attributed to natural forcings alone, because this is not the only difference between the two groups.

[5] Here we use outputs of targeted forcing experiments from two coupled climate models, NCAR PCM1 [*Meehl et al.*, 2004] and CSIRO Mk3A [*Cai et al.*, 2006], to address these issues. These targeted experiments are designed to separate the impact of increasing anthropogenic aerosols and natural forcing within both models.

2. Observational Estimates and Targeted Experiments

[6] Observed trends in globally depth-integrated OHC (from the surface to 2000 m) are based on historical ocean temperature measurements subject to bias corrections and updates. Estimates from *Levitus et al.* [2009] for 0–700 m (1955–2009)

[1]CSIRO Marine and Atmospheric Research, Aspendale, Victoria, Australia.
[2]National Center for Atmospheric Research, Boulder, Colorado, USA.
[3]Bureau of Meteorology Research Centre, Melbourne, Victoria, Australia.
[4]CSIRO Marine and Atmospheric Research, Hobart, Tasmania, Australia.

0094-8276/10/2010GL044399

[1]Auxiliary materials are available in the HTML. doi:10.1029/2010GL044399.

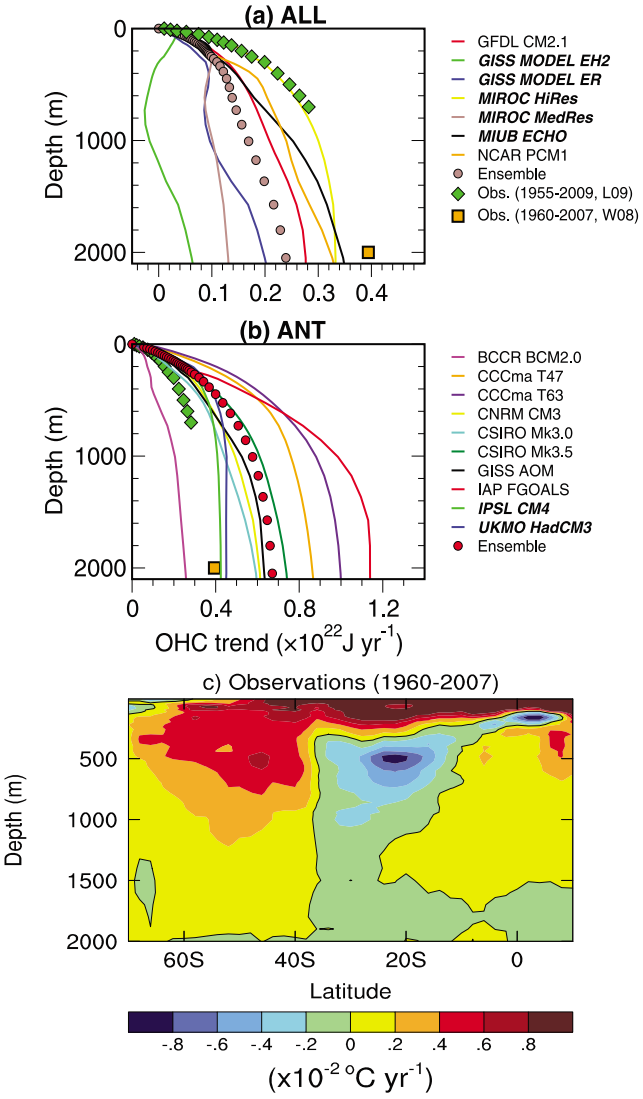

Figure 1. Depth-accumulative global OHC trends over 1951–1999, averaged over CMIP3 model experiments with (a) all forcings (ALL), and (b) with anthropogenic forcings (ANT) only (i.e., without natural forcings). Models with the indirect effect of aerosols are in bold italics. (c) Trends of zonally averaged temperature from the surface to 2000 m from observations described by *Wijffels et al.* [2008]. The green diamonds in Figures 1a and 1b are the observed OHC trends over 1955–2009 from *Levitus et al.* [2009] (L09 in Figure 1a), whereas the orange square is the observed estimate from *Wijffels et al.* [2008] (W08 in Figure 1a).

and from *Wijffels et al.* [2008] for the upper 2000 m (1960–2007) are shown in Figure 1 (further details are provided in the auxiliary material). The upper 700 m observations match well with the previous estimates of *Domingues et al.* [2008].

[7] One of the most prominent features of global ocean temperature changes over the past decades is a concentrated warming extending from the surface to around 1000m depth over the Southern Hemisphere (SH) mid-latitude ocean, accompanied by a subsurface cooling to the north [*Gille*, 2008; *Cai et al.*, 2010]. This is seen in the *Wijffels et al.* [2008] observations (Figure 1c). Such a structure is supported by a poleward shift in the midlatitude gyre circulation and the Antarctic Circumpolar Current [*Cai et al.*, 2005; *Suzuki et al.*, 2005; *Gille*, 2008; *Cai et al.*, 2010]. This feature provides an excellent benchmark for evaluating the relative importance of increasing anthropogenic aerosols and natural forcing in driving the temperature changes.

[8] Experiments from the CSIRO Mk3A and NCAR PCM1 are forced with 20th century forcings, commencing from control experiments that have been run for many centuries to ensure a quasi-steady deep ocean state. Experiments from the CSIRO Mk3A include an eight-member ensemble with ALL (with both the direct and indirect effect of anthropogenic aerosols), another eight-member ensemble with ALL eXcept increasing anthropogenic Aerosols (AXA), and a set of four NAT experiments (forced jointly with volcanic aerosols and solar variability). Therefore the impact of increasing anthropogenic aerosols is derived from the difference between the ALL and AXA ensembles as this the only difference in the model runs. The NCAR PCM1 ensembles used here include a suite of increasing anthropogenic aerosols (AER, direct effect only), NAT, and ALL; each of these ensembles has four members. The corresponding AXA ensemble is appropriately constructed as the difference between the ALL and AER ensembles, again because the presence of increasing anthropogenic aerosols is the only difference. An assumption is that aggregated globally the responses to individual forcing factors are linearly additive. The approach is shown to be valid by previous studies [e.g., *Meehl et al.*, 2004]. Time series of the anthropogenic aerosol-induced OHC confirms the linear nature of the evolution (see Figure S1 of the auxiliary material).

[9] A comparison of the ALL ensembles between the two models allows us to gauge the impact of the indirect effect of aerosols, assuming that individual model dynamics are similar. In addition, an ANT ensemble is constructed as the difference between the ALL and NAT ensembles. Before analysis, the drift in the targeted model experiments is removed using the corresponding pre-industrial control runs. Below, we compare ALL, ANT, and AXA ensembles to examine the relative importance of anthropogenic aerosols and natural forcing in terms of impacts on the global OHC trend and the associated spatial structure of ocean temperatures.

3. Linear Trends in Global OHC and the Structure of Ocean Temperatures

[10] The targeted model OHC trends in the ALL ensembles are somewhat weaker than the observed estimates (Figure 2a). The uncertainty range is estimated as the one-standard deviation of the model spread. The trend in the Mk3A is about 40 ± 15% smaller in the upper 2000 m. The PCM1 fits the observed estimates more closely with a trend that is about 18 ± 12% smaller. However, the trends in the AXA ensembles (Figure 2b) are far too strong, up to 50–75% greater than the observed, highlighting the primary importance of anthropogenic aerosols. The ANT ensembles show mixed results (Figure 2c): the ensemble-mean trend in the PCM1 is about 5% greater than observed estimates (although not significant when error estimates are included), whereas the ensemble-mean trend in the Mk3A is 20 ± 12% smaller.

[11] The forcing of anthropogenic aerosols is important for reproducing the observed subsurface cooling at SH subtropical latitudes (comparing Figures 2d and 2e with Figure 1c). By contrast, without natural forcing (i.e., ANT ensemble),

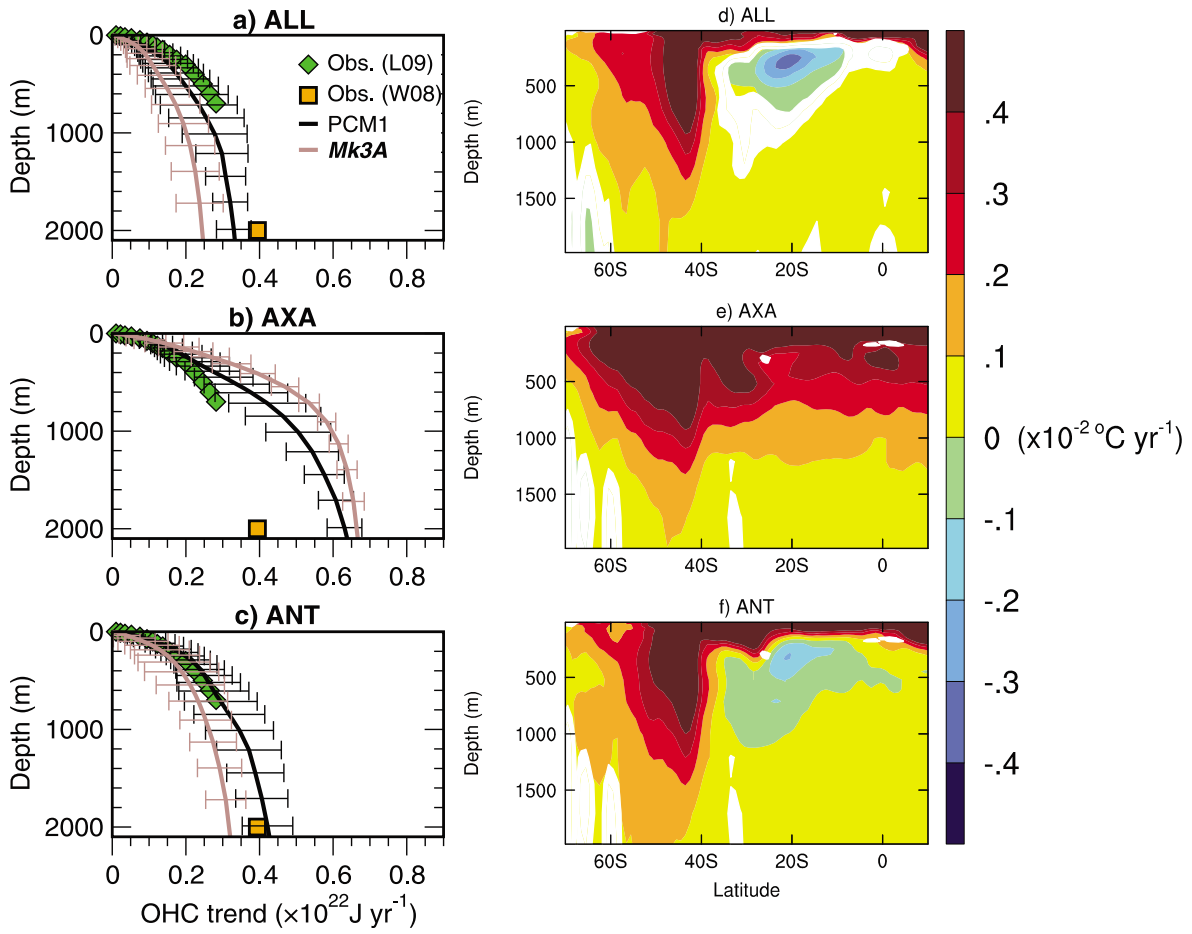

Figure 2. Depth-accumulative OHC trends over 1951–1999 for the PCM1 and the Mk3A due to (a) ALL, (b) ALL except for anthropogenic aerosols (AXA), and (c) ANT. The error bars show the 1-standard deviation of the model spread. (d–f) The trends of zonally averaged temperature from the surface to 2000 m for ALL, AXA and ANT, respectively, averaged over the two models. Coloured contours indicate where the trends are significant at the 95% confidence level.

the temperature structure changes very little (comparing Figures 2d and 2f). Thus, the forcing of increasing anthropogenic aerosols has a stronger influence than natural forcing on the structure of ocean temperature changes in the SH. Note that although the influence from natural forcing in the two targeted models is almost identical (Figure 3a), the cooling generated by anthropogenic aerosols is rather different, more than 40% greater in the Mk3A than in the PCM1 (Figure 3b). One such contributing factor to the difference is the inclusion of the indirect effect of aerosols in the Mk3A simulations, providing an extra source of cooling. In terms of temperature structure, the subtropical cooling in the Mk3A is far greater than in the PCM1, and covers all SH latitudes from the surface to beyond 1000 m (Figures 3c and 3d), where the temperature pattern is less well-defined. However, both models produce the subtropical subsurface cooling as in the observations (Figure 1c).

4. Associated Dynamical Process

[12] How is the subsurface cooling generated? Increasing anthropogenic aerosols mitigate the global Conveyor from an increasing CO_2-induced slow-down, generating a greater oceanic heat transport from the SH to the Northern Hemisphere [*Cai et al.*, 2006]. The stronger cross-hemispheric heat transport in the ALL ensemble is carried out by an intensification of the upper branch of the Conveyor, with an increasing Indonesian Throughflow, Agulhas outflow and retroflection, and strengthening flows toward the North Atlantic. Indeed, the entire SH supergyre intensifies, consistent with the notion that the supergyre is interconnected with the Conveyer [*Speich et al.*, 2007]. The heat for supporting the stronger Conveyor is derived mainly along the Conveyor pathway in the latitude band 10°S–35°S, leading to a substantial cooling in the subtropical-midlatitude South Atlantic, which in turn draws heat along the pathway of the Agulhas outflow and the Indonesian Throughflow, inducing the cooling in the SH off-equatorial Indo-Pacific waters [see *Cai et al.*, 2006, Figure 4]. *Stenchikov et al.* [2009] show a similar pan-oceanic adjustment process in response to a volcanic aerosol-induced cooling, in which the Conveyer circulation intensifies and the temperature change is not uniformly distributed.

[13] The intensification of the supergyre is accompanied by a stronger SH midlatitude poleward heat transport; this moves the location of the maximum sea surface temperature gradients (not shown) as well as shifting the maximum atmospheric baroclinicity polewards [*Cai and Cowan*, 2007;

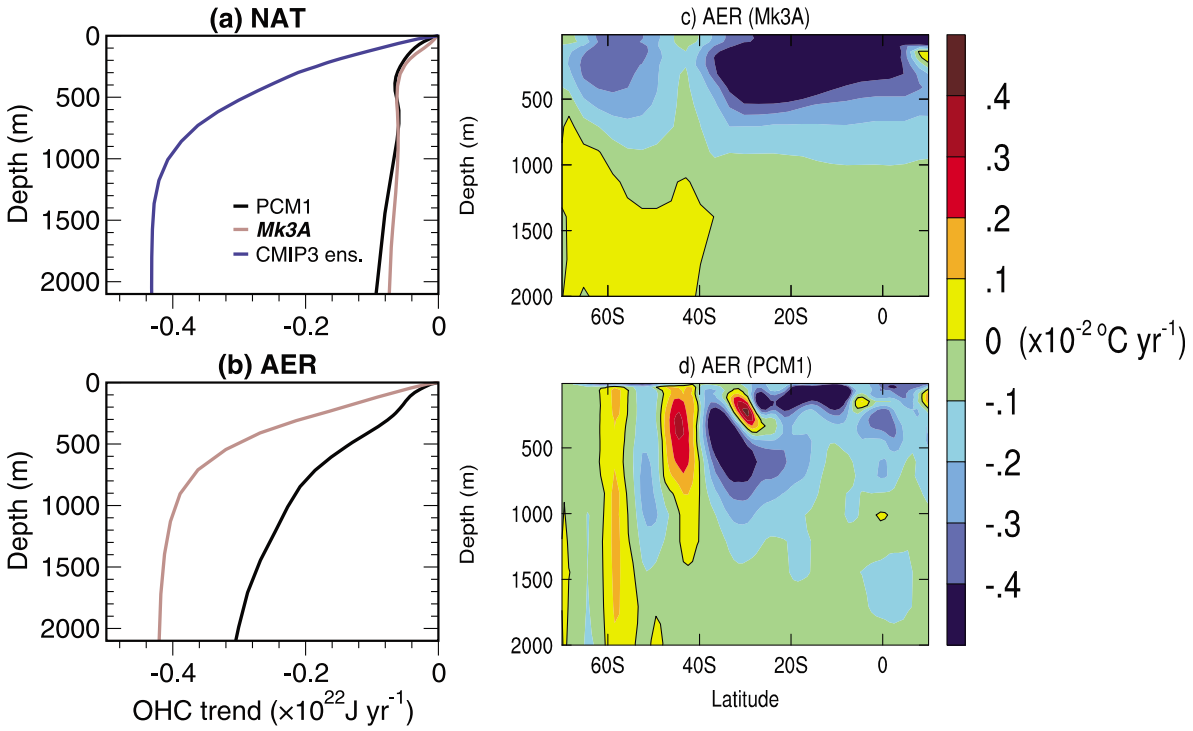

Figure 3. Depth-accumulative OHC trends over 1951–1999 for the PCM1 and the Mk3A due to (a) natural forcing (NAT), and (b) anthropogenic aerosols (AER). Also shown in Figure 3a is the OHC trend due to the difference in the CMIP3 ALL and ANT ensembles in Figures 1a and 1b. (c and d) trends of zonally averaged temperature induced by anthropogenic aerosols for the Mk3A and PCM1, respectively.

Simmonds and Lim, 2009]. This reduces the frequency of storms in the midlatitudes, however more events occur to the south. In association, westerlies to the north weaken but strengthen to the south, as storm activity shifts poleward, with a Southern Annular Mode (SAM)-like pattern of changes. In both models, the SAM-like trend is stronger in the ALL ensembles than in the AXA ensembles, and tends to be located further to the south (Figure 4), although the sizes of the trend between the two models are substantially large. These wind changes and the associated positive curls in turn reinforce a poleward intensifying SH subtropical ocean circulation [*Cai et al.*, 2005; *Cai and Cowan*, 2007].

5. Discussion

[14] Our targeted experiments provide useful insights in terms of interpreting CMIP3 ensemble results. The two

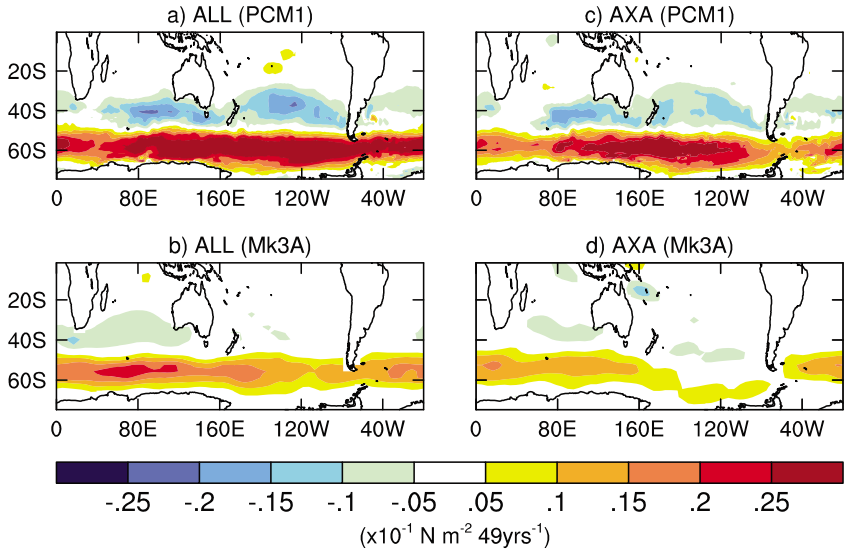

Figure 4. Trends of zonal wind stress over 1951–1999 for the ALL ensembles of (a) PCM1 and (b) Mk3A. (c and d) Trends of AXA ensembles from the same models.

CMIP3 ensembles shown in Figures 1a and 1b are stratified in terms of whether natural forcing (predominantly volcanic aerosols) is included or not. Many studies [e.g., *Domingues et al.*, 2008] have noticed that only in the subgroup with natural forcing (mainly volcanic) can more realistic global OHC and temperature trends be simulated; without natural forcing, the trend is far too large. Our analysis suggests that the improvement is not just due to the inclusion of natural forcing alone. The difference between the CMIP3 ALL ensemble and CMIP3 ANT ensemble (Figure 3a, blue curve), if attributed to natural forcing, would highly contravene the results of our targeted experiments; the difference is about five times as large as the NAT ensembles in the targeted models. Further, the difference is equivalent to a heat flux forcing of -0.45 W m^{-2} applied to the ocean surface ($\simeq 3.3 \times 10^{14}$m^2) over the 49-year period, many times larger than the estimate for natural forcing in the Intergovernmental Panel on Climate Change (IPCC) Fourth Assessment Report [*Forster et al.*, 2007].

[15] The indirect aerosol effect has a mean and uncertainty range in its radiative forcing of -0.7 [-1.8 to -0.3] W m^{-2}, and the direct effect is in the range of -0.5 [-0.9 to -0.1] W m^{-2} [*Forster et al.*, 2007]. The large range in the mean of either the direct or the indirect effect makes it a likely cause for the difference between the two CMIP3 ensembles. It turns out that there is a built-in systematic difference between the two ensembles: there are five models (out of seven) in CMIP3 ALL ensemble (Figure 1a) that incorporate both the direct and indirect effect of anthropogenic aerosols, whereas in the ANT ensemble there are only two (out of 10) that include the indirect effect. Although the two ensembles are stratified by natural forcing, models that incorporate natural forcing, and therefore with the sophistication of incorporating the impact of volcanic aerosols, tend to also include the indirect effect, which is an additional cooling. Stratifying models on the basis that they include both aerosol effects or the direct effect-only reproduces much of the difference shown in Figures 1a and 1b.

[16] Given that this built-in systematic difference is mainly responsible for the under-estimated trend shown in Figure 1a, it follows that the indirect effect is over-estimated, with significant implications for climate projections using these models. For example, in IPCC scenarios in which anthropogenic aerosols are projected to continue to increase in the upcoming decades (e.g., SRES A2, until 2030), this bias would mean an underestimation in the projected steric sea level rise.

6. Conclusions

[17] A subgroup of CMIP3 20th century experiments with all forcing factors produces a global OHC trend since 1951–1999 that is too weak when compared with the observed, whereas another subgroup without natural forcings overestimates the global OHC trend. Given that both anthropogenic and volcanic aerosols induce an oceanic cooling, the present study examines their respective role in the global OHC trends and in the structure of the ocean temperature changes. This is achieved using targeted experiments from two models, which allow a clean separation of the impacts of individual forcing components within each model. We find that natural forcing is unlikely to account for the bulk of the difference between the two CMIP3 ensembles; one such reason could be the overestimated cooling of the indirect aerosol effect. Further, the forcing of increasing anthropogenic aerosols has a far greater influence on the structure of the simulated ocean temperature changes and on the global OHC trends than natural forcing. In both models, the greater impacts from increasing anthropogenic aerosols include a concentrated cooling in the SH subtropical latitudes, as a result of a more stable Conveyor, a poleward intensification of the super-gyre circulation, and a stronger SAM.

[18] **Acknowledgments.** We thank the modelling team at NCAR for the provision to use the PCM1 simulations, and Leon Rotstayn and Martin Dix for generating the Mk3A targeted experiments. Portions of this study were supported by the Office of Science (BER), U. S. Department of Energy, Cooperative Agreement No. DE-FC02-97ER62402, and the National Science Foundation. The National Center for Atmospheric Research is sponsored by the National Science Foundation.

References

Cai, W., and T. Cowan (2007), Impacts of increasing anthropogenic aerosols on the atmospheric circulation trends of the Southern Hemisphere: An air-sea positive feedback, *Geophys. Res. Lett.*, *34*, L23709, doi:10.1029/2007GL031706.

Cai, W., G. Shi, T. Cowan, D. Bi, and J. Ribbe (2005), The response of the Southern Annular Mode, the East Australian Current, and the southern mid-latitude ocean circulation to global warming, *Geophys. Res. Lett.*, *32*, L23706, doi:10.1029/2005GL024701.

Cai, W., D. Bi, J. Church, T. Cowan, M. Dix, and L. Rotstayn (2006), Pan-oceanic response to increasing anthropogenic aerosols: Impacts on the Southern Hemisphere oceanic circulation, *Geophys. Res. Lett.*, *33*, L21707, doi:10.1029/2006GL027513.

Cai, W., T. Cowan, S. Wijffels, and S. Godfrey (2010), Simulations of processes associated with the fast warming rate of the southern Midlatitude Ocean, *J. Clim.*, *23*, 197–206.

Domingues, C. M., J. A. Church, N. J. White, P. J. Gleckler, S. E. Wijffels, P. Barker, and J. R. Dunn (2008), Upper-ocean warming and sea-level rise, *Nature*, *453*(7198), 1090–1096.

Forster, P., et al. (2007), Changes in atmospheric constituents and in radiative forcing, in *Climate Change 2007: The Physical Science Basis. Contribution of Working Group I to the Fourth Assessment Report of the Intergovernmental Panel on Climate Change*, edited by S. Solomon et al., pp. 129–234, Cambridge Univ. Press, Cambridge, U. K.

Gille, S. T. (2008), Decadal-scale temperature trends in the Southern Hemisphere ocean, *J. Clim.*, *21*, 4749–4765.

Levitus, S., J. I. Antonov, T. P. Boyer, R. A. Locarnini, H. E. Garcia, and A. V. Mishonov (2009), Global ocean heat content 1955–2008 in light of recently revealed instrumentation problems, *Geophys. Res. Lett.*, *36*, L07608, doi:10.1029/2008GL037155.

Liepert, B. G., J. Feichter, U. Lohmann, and E. Roeckner (2004), Can aerosols spin down the water cycle in a warmer and moister world?, *Geophys. Res. Lett.*, *31*, L06207, doi:10.1029/2003GL019060.

Meehl, G. A., W. M. Washington, C. M. Ammann, J. M. Arblaster, T. M. L. Wigley, and C. Tebaldi (2004), Combinations of natural and anthropogenic forcings in twentieth-century climate, *J. Clim*, *17*, 3721–3727.

Nazarenko, L., and S. Menon (2005), Varying trends in surface energy fluxes and associated climate between 1960 and 2002 based on transient climate simulations, *Geophys. Res. Lett.*, *32*, L22704, doi:10.1029/2005GL024089.

Simmonds, I., and E.-P. Lim (2009), Biases in the calculation of Southern Hemisphere mean baroclinic eddy growth rate, *Geophys. Res. Lett.*, *36*, L01707, doi:10.1029/2008GL036320.

Speich, S., B. Blanke, and W. Cai (2007), Atlantic meridional overturning circulation and the Southern Hemisphere supergyre, *Geophys. Res. Lett.*, *34*, L23614, doi:10.1029/2007GL031583.

Stenchikov, G., T. L. Delworth, V. Ramaswamy, R. J. Stouffer, A. Wittenberg, and F. Zeng (2009), Volcanic signals in oceans, *J. Geophys. Res.*, *114*, D16104, doi:10.1029/2008JD011673.

Suzuki, T., H. Hasumi, T. T. Sakamoto, T. Nishimura, A. Abe-Ouchi, T. Segawa, N. Okada, A. Oka, and S. Emori (2005), Projection of future sea level and its variability in a high-resolution climate model: Ocean processes and Greenland and Antarctic ice-melt contributions, *Geophys. Res. Lett.*, *32*, L19706, doi:10.1029/2005GL023677.

Wijffels, S., J. Willis, C. Domingues, P. Barker, N. White, A. Gronell, K. Ridgway, and J. A. Church (2008), Changing expendable bathythermograph fall rates and their impact on estimates of thermosteric sea level rise, *J. Clim.*, *21*, 5657–5672.

J. M. Arblaster, Bureau of Meteorology Research Centre, 700 Collins St., Melbourne, Vic 3001, Australia.

W. Cai and T. Cowan, CSIRO Marine and Atmospheric Research, PMB 1, Aspendale, Vic 3195, Australia. (wenju.cai@csiro.au)

S. Wijffels, CSIRO Marine and Atmospheric Research, GPO Box 1538, Hobart, Tas 7000, Australia.